

Observations on the Transiting Planet around KOI1152

Muxue Liu

A senior thesis submitted to the faculty of
Brigham Young University
in partial fulfillment of the requirements for the degree of

Bachelor of Science

Denise Stephens, Advisor

Department of Physics and Astronomy

Brigham Young University

April 2012

Copyright © 2012 Muxue Liu

All Rights Reserved

ABSTRACT

Observations on the Transiting Planet around KOI1152

Muxue Liu

Department of Physics and Astronomy

Bachelor of Science

On July 24th 2011, the Department of Physics and Astronomy of Brigham Young University observed the transiting exoplanet around object KOI1152, a Sun-like star imaged previously by NASA's Kepler telescope. After data reduction, clear light curves are obtained, which confirm the nature of the transiting object as a planet. The amount of magnitude decrease (~ 0.1 mag) agrees with the predicted value published by the Kepler team.

Keywords: exoplanet, transit, Kepler mission, photometry, data reduction, aperture photometry, differential photometry, light curve

ACKNOWLEDGMENTS

First of all, I would like to express my gratitude to the Department of Physics and Astronomy of Brigham Young University for providing me a good environment to learn and develop.

Then I wish to express my respect and appreciation to all the faculty members in our department for the excellent example they have set for me as dedicated scientists and responsible educators. I would like to thank my research advisor Dr. Denise Stephens in specific for the knowledge and skills she has taught me. And I want to thank my colleague Joseph Rawlins who has been working in the same research team with me for sharing his valuable experience.

Finally, I would like to thank my family in China for their support both financially and spiritually through the years I have been studying in the United States.

Contents

Table of Contents	vii
List of Figures	ix
1 Background	1
1.1 Exoplanets	1
1.2 Kepler Mission	2
2 Methodology	5
2.1 Instruments	5
2.2 Data Reduction	5
2.2.1 Locate object and select ensemble stars	6
2.2.2 Check for drift in coordinates	6
2.2.3 Aperture Photometry	7
2.2.4 Differential Photometry	8
2.2.5 Magnitude Correction and Error Calculation	9
3 Results and Conclusions	11
3.1 Light Curves	11
3.2 Functional Fits	14
4 Overview to Next Stage	17
Bibliography	19
Index	19

List of Figures

3.1	Light profile for the I-filter	12
3.2	Light profile for the V-filter	12
3.3	Three most likely astrophysical mimics	13
3.4	Functional fit to the I-filter data	14
3.5	Functional fit to the V-filter data	15
3.6	Limb darkening effect	16

Chapter 1

Background

1.1 Exoplanets

Exoplanets, or extrasolar planets, are planets outside the solar system. Astronomers have intended to observe them since the 19th century, but because of the limitation of instruments, their existence was not confirmed until 1992. Since then, more of these objects have been detected, and it is now believed that many stars have planetary systems around them, just like our solar system.

Depending on their mass, exoplanets exhibit various characters. There is now probable evidence for substantial numbers of three types of exoplanets: gas giants, hot-super-Earths, and ice giants, all in short period orbits (NASA Last Modified: 06 Apr 2012). No conclusion has been made concerning the absolute abundance of each type, although the data released by the Kepler mission indicates that a majority of the sample falls between 1.25 to 15 Earth-radii (Borucki et al. 2011). However, this phenomenon is possibly due to selection bias due to the limitation of detection techniques.

Because the photons emitted by exoplanets are extremely few compared to the stars they orbit, it is almost impossible to image them directly. Instead, they are detected by the method of transit.

The term transit refers to the passage of a planet across the stellar meridian (Zeilik & Gregory 1998). A main sequence star should be relatively constant in flux over time. That is, when we record its flux with respect to time, it should be a flat line. However, if there is a planet orbiting it, its light profile will change due to the presence of the planet. Whenever the planet passes in front of the star's hemisphere that is facing the telescope, it blocks a fraction of the star's light. As a result, there will be abrupt decreases or so-called “dips” in the light profile, which occurs periodically.

1.2 Kepler Mission

On March 6, 2009, NASA launched the Kepler mission. It is a discovery-class mission designed to determine the frequency of Earth-size planets in and near the habitable zone of solar-type stars. The term habitable zone refers to the region where planetary temperatures are suitable for water to exist on a planet's surface (Borucki et al. 2011). The optical instrument on the Kepler mission is a Schmidt telescope with a 0.95-meter aperture and a 105 square degree field of view. This is comparable to the area of sky covered by a person's hand held at arm's length. Although it may seem small compared to the size of the entire telescope, it is actually a very large field of view for astronomical telescopes. Such a large field is required to stare at a large enough number of stars to have any possibility of detecting just one Earth-size planet. During the life of the mission (3.5 or more years), the telescope will be able to observe more than 100,000 stars (NASA Last Modified: 06 Apr 2012). Kepler has been observing a $\sim 115 \text{ deg}^2$ region of sky, monitoring $\sim 165,000$ sources every 29.4 minutes with unprecedented stability ($<0.1\%$ for a 15^{th} magnitude source) and high ($>90\%$) duty cycle over a period of years (R.F.Mushotzky et al. 2011). On February 1st, 2011, it released data for 156,453 stars observed from May 2nd to September 16th, 2009. 1235 planetary candidates with transit-like signatures, which are associated with 997 host stars, are detected in this period. A study published in July, 2011 separated 1217 planetary candidates into 5 class sizes:

68 Earth-size, 288 super-Earth-size, 662 Neptune-size, 165 Jupiter-size, and 19 up to twice the size of Jupiter (Borucki et al. 2011). These are all planetary candidates. Further observations by other telescopes are needed to clarify that they actually are planets.

Chapter 2

Methodology

2.1 Instruments

Object KOI1152 (RA=19:46:47, Dec=47:19:38) is one of the objects identified as a planetary candidate by Kepler. Data on this object was taken in the West Mountain Observatory (WMO) on July 24th of 2011 by Dr. Michael Joneer. The 0.9-m Telescope was used. The telescope has an f-ratio of 5.5 and a plate scale of 41"/mm. It was attached to a Finger Lakes PL-09000 CCD system with 12 μ m pixels in a 3056 by 3056 array, which gave a 25.2'×25.2' field of view. Johnson/Cousins I and V filters were used for imaging, and 51 frames were taken in each of the filters with an exposure time of 45 seconds per frame.

2.2 Data Reduction

All the data from WMO were saved to the BYU Kepler archive after the completion of zero frame correction, dark frame correction, and flat field correction by the West Mountain staff. When students download data from the archive, they generally follow a 5-step procedure to reduce data:

2.2.1 Locate object and select ensemble stars

The first thing is to locate the object. In IRAF, we use the command IMHEADER to view the RA and Dec of the object. Then on the Digitized Sky Survey website, retrieve the image, and compare it to the image displayed in DS9. Note that these two images are symmetric about the origin. And the digitized Sky Survey always put the object at the center of the image. Look for patterns in the images and match them. For future convenience, print out the image and mark the object as star #1.

The next thing is to select the ensemble stars. Generally speaking, a larger sample will give a more accurate result in the differential photometry step. In the case of KOI1152, the field contains abundant stars, and 72 of them were selected. Note that you should only select objects that are considered "normal stars", which excludes stars with light saturation, visual binary stars, stars hit by cosmic rays, and galaxies. You can tell from the image that "normal stars" appear as clear circular spots. To do it more accurately, use command IMEXAM to view the elongation and surface plot of each star. "Normal stars" should have relatively small elongations and sharp Gaussian-shape surface plots. Exclude objects with large elongations. If the surface plot is flattened on the top, then the star is saturated and should be excluded. If the surface plot has two peaks, then the object is likely a binary and should also be excluded. In the end of the selection process, mark all the selected ensemble stars on the printed image, and number them accordingly.

2.2.2 Check for drift in coordinates

It is important to check the consistency in coordinates from image to image. To do this, display a few frames in DS9 and blink them. If you see a trend of motion of the entire field, that means the telescope was not tracking the stars. This happened to the case of KOI1152. Because there were 51 frames in each filter and 73 marked stars in each frame, it was almost impossible to manually record the coordinates of each of them. The best thing to do was to record the coordinates in the

first image, and then find the trend of change in coordinates and fix it for the rest of the frames.

We started with the I-filter. We chose three stars (star #12, #15, and #31), wrote down their coordinates in each frame, and subtracted each coordinate value with the value in the first frame. For example, the x and y coordinates of star #12 in the first frame was (1438.01, 1623.05); in the second frame it was (1437.13, 1625.34). So the shift of #12 in the second image was (-0.88, 2.29). We did this for each image. Then we separately added up the shifts in x-coordinates and y-coordinates of stars #12, #15, and # 31, and divided by 3. The results were the average shifts of every star in that frame. For example, in the third frame, the shifts were (-1.52, 3.24) for # 12, (-2.24, 3.27) for #15, and (-1.58, 3.36) for # 31. So in this frame, the average shift of every star in x was -1.78, and the average shift in y was 3.29. We did this for each frame. In the end, we got average shifts in x and y for stars in all 51 images in the I-filter. The same procedure was repeated for the V-filter.

We subtracted the average shifts in x and y coordinates from each star in each frame to get the fixed coordinates. A coordinate file was created for each frame, and the correction procedure was completed.

2.2.3 Aperture Photometry

The term photometry means the measurement of photons. There are a number of methods to do photometry, and the simplest one is aperture photometry. An aperture is an angular area around a point. Aperture photometry is literally the counting of each photon in a circular aperture that hits the detector. To use this method, we first determine the profile of each star of how light spreads out due to refraction and diffraction by the atmosphere and telescope. Then we place an annulus around the profile. Finally we sum up the counts inside that aperture and subtract the counts from the sky to get the total counts from the star. This count corresponds to the number of photons received from the star.

To do this in IRAF, first go to NOAO. Open package DIGIPHOT, and then APPPHOT, which stands for aperture photometry. The program PHOT is the one to be used. Type: phot (image name) ""coords=(coordinate file name). For example: phot KOI1152-001I.fits ""coords=i1coord.txt. Do this on each image. A "mag.fits" file will be created for each image when it is done.

The "mag.fits" files contain information such as filter, airmass, and observation time, which are data from the image headers. Most importantly, they contain magnitudes of different aperture sizes ranging from 2 to 11 pixels in step of 0.5. Our task is to decide which aperture size we are going to use. For each "mag.fits" file, we extract magnitudes of all aperture sizes, plot the magnitudes versus aperture size, and observe where the curve starts to flatten out. Physically, it means at this aperture size, the annulus includes all the light from the star. Do this for each image, and see where the average cutoff aperture size is. In our case, it was at aperture size 2.5. Therefore we were going to use the magnitudes at this size in further reduction.

Note that aperture photometry is not suitable for crowded fields. If the field is very closely packed, it is better to use other photometry packages such as DAOPHOT.

2.2.4 Differential Photometry

In Step 1 we selected our ensemble stars. In this step we use those stars to perform differential photometry. The basic idea of differential photometry is to measure the instrumental magnitudes of the ensemble stars, take an average, and subtract the average from the magnitudes.

There are different methods to do differential photometry. In our case we used VARSTAR version 5, a program written in C by BYU students under the instruction of Dr. Eric Hintz. To begin with, you need to create an input file for the program, which contains information from the "mag.fits" files. Use the following command: `txdump *.mag.1 id,mag[aperture size],otime,xairmass,ifilter > (filename).lst`. For example, we used `"txdump *.mag.1 id,mag[2],otime,xairmass,ifilter > inputi.lst"` for the I-filter.

With the “.lst”file you are ready to run VARSTAR. The program takes the input file, and iterates through the field of stars to eliminate those with large errors. When you execute the program, it displays the object number and their error. Ideally, the error should be close to 0.007. You are going to eliminate the target star (object #1) and large-error objects. Each time you eliminate 5 to 8 objects, and you repeat the process several times until when you have at least 7 objects left with error values close to 0.007.

After the elimination process, a “.sup”file will be created for each of your objects. These files contain instrumental magnitudes of each star. In IRAF, you can use the command PLOT to generate a light curve for each star. At this point, you are able to tell whether the signals of transit are resolvable.

2.2.5 Magnitude Correction and Error Calculation

To obtain the true magnitudes, we need to calculate the extinction and zero point. Along with the object frames, there were a set of standard star frames taken the same night using the same telescope configuration. We performed the previous reduction procedure on those standard fields, and extracted the magnitudes and airmass values from the "mag.fits" files. If we were to plot the magnitudes versus airmass, the slope of the curve would be the extinction. And the true magnitudes could be calculated using equation

$$m_0 = m_i - \text{airmass} \times \text{extinction} + \text{zeropoint}. \quad (2.1)$$

Unfortunately, our standard data set were taken at only 2 airmass values, which was insufficient to determine the slope. Therefore, we did not do the extinction correction on our data. We just corrected the zero point, which gave the actual apparent magnitude of our star compared to Vega.

We calculated the error in magnitudes using the standard fields. We extracted the magnitudes from the standards“mag.fits”files, and compared them with the Landolt Equatorial Standards’values. We found the differences between the values for each filter, and calculated the

standard deviation. Label this value as $\sigma_{zeropoint}$. Then we went back to the object frames, and extracted the MERR MAG values from their "mag.fits" files, which were standard deviation of the observed magnitudes. The error in real magnitudes, labeled as σ , can be calculated from

$$\sigma = \sqrt{\text{MERR MAG}^2 - (\sigma_{zeropoint})^2}$$

Chapter 3

Results and Conclusions

3.1 Light Curves

At the error correction stage, we found that the zero point in magnitude was -3.929 for the I-filter, and it was -3.018 for the V-filter. The real magnitude is the observed value subtracted by the zero point. After the subtraction, we plotted the light curves of the real magnitudes versus HJD for the I and V filters separately as shown in Figure 3.1 and Figure 3.2.

In the official Kepler database, the decrease in depth (ppm) of KOI1152 due to the transiting planet is 82516. Using the conversion $m = |2.5 \times \text{Log}(1 - 10^{-6}) \times \text{depth}|$, the decrease in magnitude is 0.0935. The average decrease in magnitude from our data is approximately 0.1 in both filters, which coincides with the predicted value.

Using Landolt's Standard stars, we found the standard deviation in zero point correction is 0.0212 in the I-filter and 0.0228 in the V-filter. Combining these with the standard deviations in magnitudes, which are 0.005 in the I-filter and 0.006 in the V-filter, we found the standard deviations in real magnitudes are 0.0218 in the I and 0.0236 in the V.

As shown in the light curves, the difference between maxima and minima in magnitude is ap-

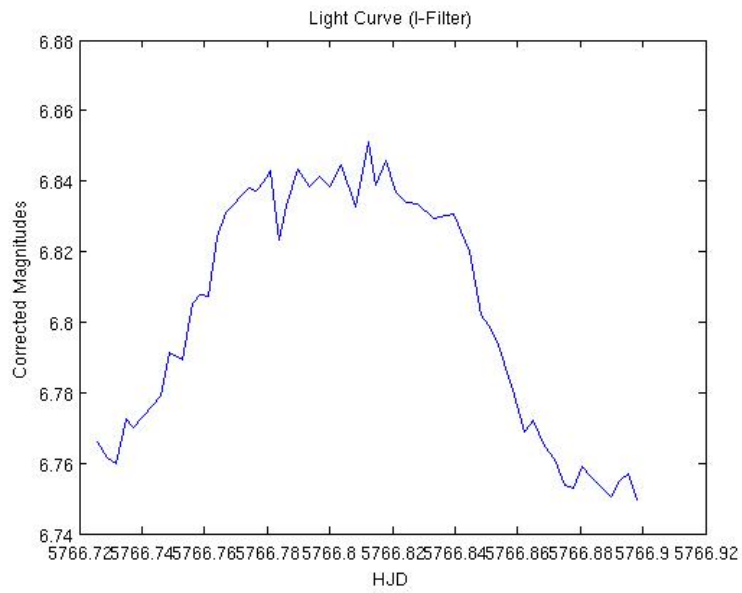


Figure 3.1 Light profile for the I-filter.

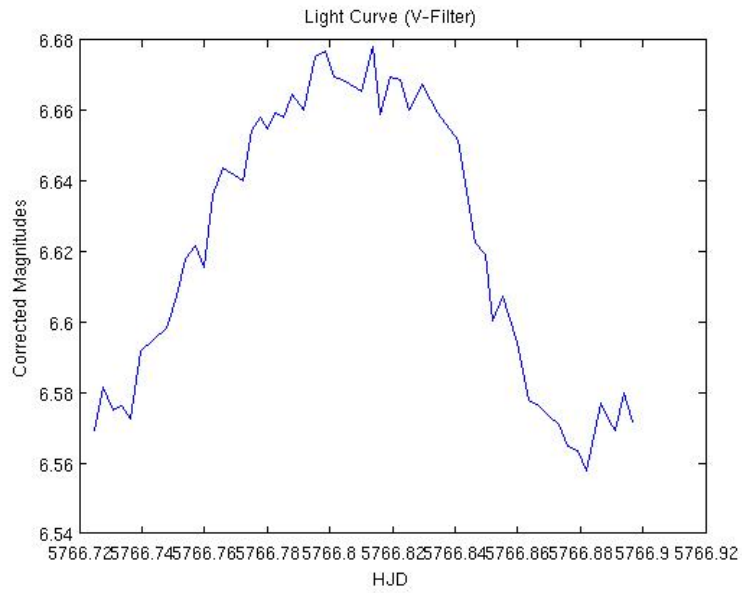


Figure 3.2 Light profile for the V-filter.

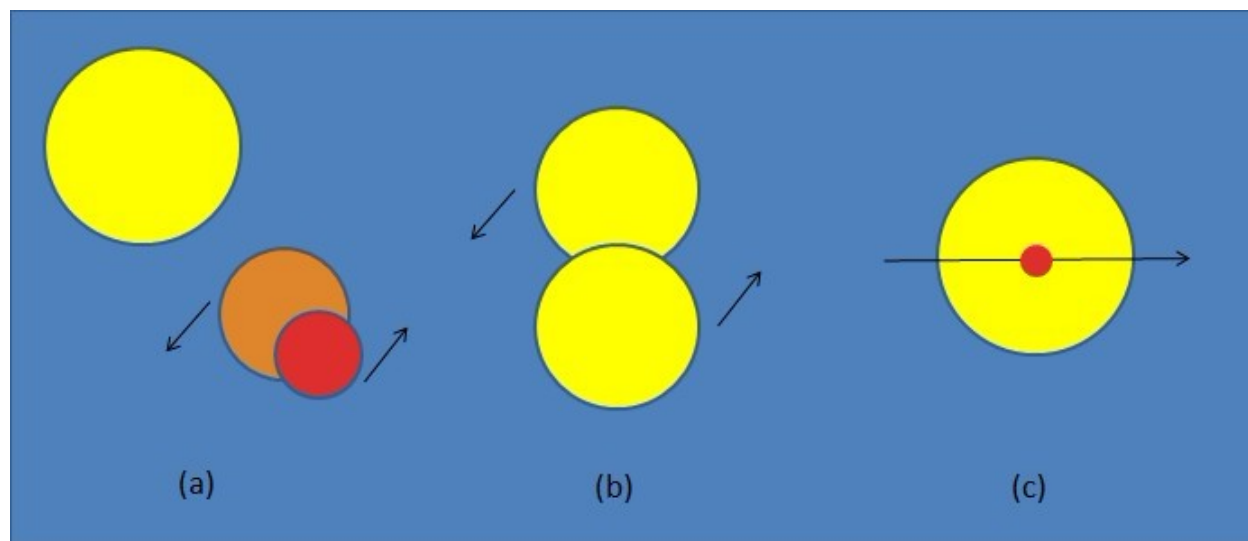


Figure 3.3 Schematic illustration of the three most likely astrophysical mimics.

proximately 0.1 in both filters with standard deviations calculated above. The coherent magnitude decrease is evidence that the transiting object is a candidate for a planet.

According to previous studies, the most common imposters identified as possible transiting planets are: (a) Blended eclipsing binary systems; (b) Grazing eclipsing binary systems with equal-mass component; (c) Transits by planet-sized objects (Haswell 2010). These three most likely astrophysical mimics are illustrated in Figure 3.3.

To determine the nature of the mechanism, different characters should be observed, such as the shape of the curve and percentage of magnitude decrease. The point we are demonstrating here is to compare the magnitude decrease in different colors. In cases (a) and (b), the light occultation is caused by dim late-type stars, and we will observe a deeper decrease in the V band than in the I band. That is because the transiting dim stars emit red to near infrared lights, which contribute to the host stars' emission in the I band. In case (c), the transiting object can be either a brown dwarf or a white dwarf. If it is a brown dwarf, then there will be a deeper decrease in V, because the brown dwarf peaks in the I; if it is a white dwarf, then there will be a deeper decrease in I, because white dwarfs peak in blue light. Since we have approximately equal amount of magnitude drop in I and

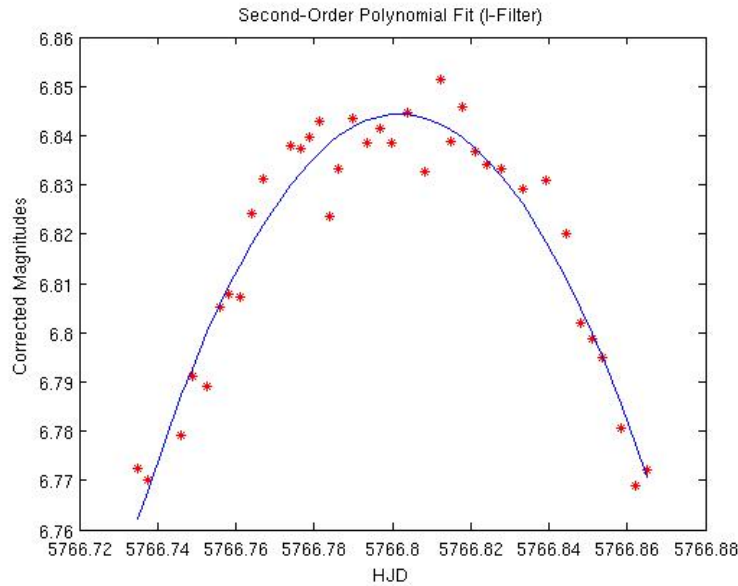


Figure 3.4 Functional fit to the I-filter data.

V, we are confident to conclude that our transiting object is a planet, whose emission peaks in the far infrared.

3.2 Functional Fits

Using Matlab, we found the 2nd-order polynomial fits to the data in each filter. We defined the ingress at the 4th data point and egress at the 40th point, and the functions were defined in this domain. In the I-filter, the functional fit was $y = -(1.84 \times 10)x^2 + (2.12 \times 10^5)x - (6.12 \times 10^8)$; and in the V-filter, it was $y = -(2.26 \times 10)x^2 + (2.61 \times 10^5)x - (7.52 \times 10^8)$. The plots are shown in Figure 3.4 and Figure 3.5.

Technically, it is more useful to fit the “transit floor” rather than the entire transiting process. By examining the flatness of the transit floor, we are able to observe the effect of stellar limb darkening.

Limb darkening refers to the phenomenon that a star's light diminishes from the center of the

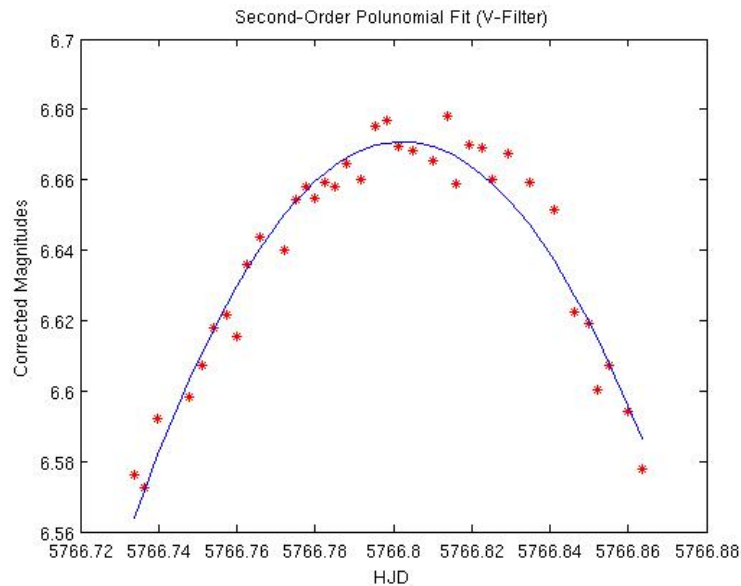


Figure 3.5 Functional fit to the V-filter data.

disk of view to the edge. Main sequence stars have out layers composed of plasma. The light that escapes from them comes from a variety of depths within the stellar atmosphere. The probability of escape of a photon emitted within a particular layer of the atmosphere is strongly dependent on the optical depth of that layer (Haswell 2010). This is the basic reason behind the darkening effect.

Figure 3.6 schematically illustrates the effect of limb darkening. If the transit floor we observe is very flat, that indicates the planet is crossing in front of the central part of the disk of view (case 1). Because the core of the disk has less darkening effect, the magnitudes observed in this region are relatively constant. On the other hand, if the transit floor has more curvature, it implies that the planet is crossing in front of the edge of the disk of view (case 2). Closer to the edge of the disk, the darkening effect is more dramatic. Therefore, when a planet transits through the limb region, the magnitudes observed will constantly vary.

Unfortunately, Matlab was not able to perform a precise fit to the transit floors in our light curves. However, the Department of Physics and Astronomy has planned to write a program that does the precise fit to the data in the summer of 2012.

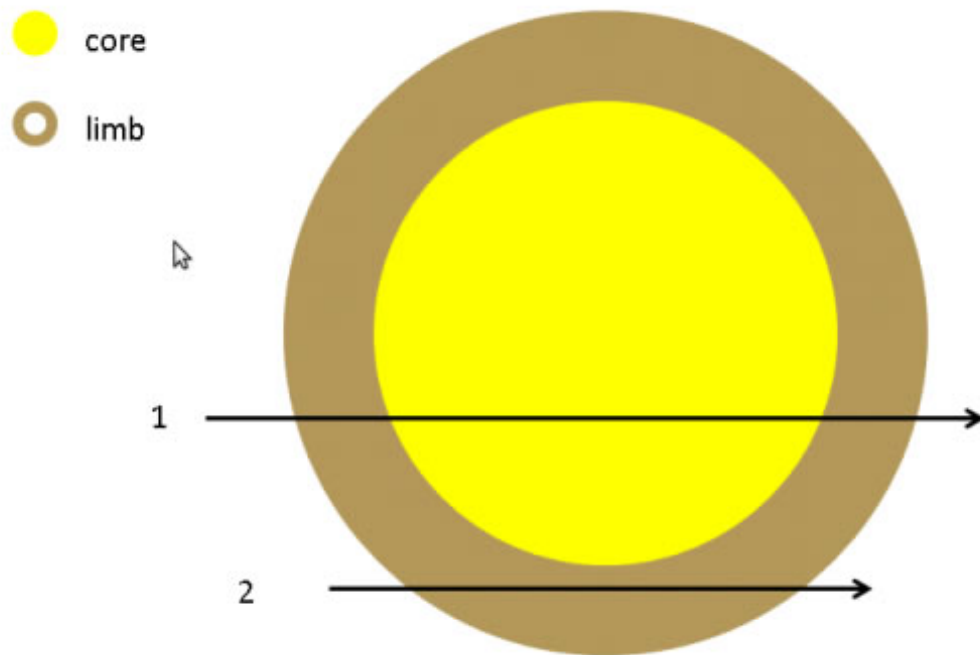


Figure 3.6 Schematic illustration of the limb darkening effect.

Chapter 4

Overview to Next Stage

In the summer of 2012, the department is going to do another observation run on object KIO1152 along with another 10 objects using the same instruments on West Mountain Observatory. We will look for agreement between new and old data to confirm the existence of the exoplanet. The department is also applying to observe on the Sophia telescope to obtain spectroscopic data, so that more details of the planetary systems can be revealed.

Bibliography

Borucki, W. J., et al. 2011, *The Astrophysical Journal*, 736, 19

Haswell, C. A. 2010, *Transiting Exoplanets* (The Edinburgh Building, Cambridge CB2 8RU, UK: Cambridge University Press)

NASA. Last Modified: 06 Apr 2012, <http://kepler.nasa.gov/>

R.F.Mushotzky, R.Edelson, W.Baumgartner, & P.Gandhi. 2011, *The Astrophysical Journal Letters*, 743

Zeilik, M., & Gregory, S. A. 1998, *Introductory Astronomy and Astrophysics*, 4th edn., ed. J. Vondeling & J. Bortel (10 Davis Drive, Belmont Drive, CA 94002, USA: Brooks/Cole, Cengage Learning)

